Thermal magnifier and external cloak in ternary component structure

Shuai Yang, Liujun Xu (iD), and Jiping Huang (iD)

View Online   Export Citation   CrossMark

ARTICLES YOU MAY BE INTERESTED IN

AIP Publishing

Thermal magnifier and external cloak in ternary component structure

View Online   Export Citation   CrossMark

Shuai Yang, Liujun Xu, [ID] and Jiping Huang[a] [ID]

AFFILIATIONS

Department of Physics, State Key Laboratory of Surface Physics, and Key Laboratory of Micro and Nano Photonic Structures (MOE), Fudan University, Shanghai 200433, China

[a]**Electronic address:** jphuang@fudan.edu.cn

ABSTRACT

Thermal metamaterials have aroused broad research interests for their potential applications in heat manipulation. Among them, bilayer thermal cloak is a representative one. However, the requirement of zero thermal conductivity of the inner layer may largely restrict broader applications. In this work, we remove the requirement of zero thermal conductivity and explore a ternary component structure. By calculating its effective thermal conductivity, we derive some special relations which result in two distinct camouflage behaviors, i.e., thermal magnifier and external cloak. Concretely speaking, thermal magnifier can thermally disguise a small object into a big one, and external cloak can thermally hide a component outside the cloak. Finite-element simulations are conducted in both two and three dimensions, which echo with our theoretical prediction. The ternary component structure has potential applications in thermal camouflage, thermal invisibility, etc. This work not only paves the way for designing camouflage in thermotics but also opens up an avenue for exploring camouflage in other diffusive fields like electrostatic, magnetostatic, and particle diffusive fields.

Published under license by AIP Publishing. https://doi.org/10.1063/1.5083185

I. INTRODUCTION

Heat energy is everywhere in nature, and hence its effective control is of great significance, especially for easing the energy issues. Fortunately, thermal metamaterials provide powerful methods to explore novel thermal phenomena, such as thermal cloak,[1–9] thermal rotator,[5,10] thermal camouflage,[11–18] thermal bending,[19–21] thermal lens,[22] etc. Among them, bilayer thermal cloak[7–9] is a representative one which largely simplifies the structure as required by transformation thermotics. However, such a design requires the thermal conductivity of the inner layer to be zero, which may limit flexible control and broader applications.

Here, we propose a ternary component structure composed of a bilayer structure (without zero thermal conductivity) and an inside object, which is what we expect to explore in this work.

We derive the effective thermal conductivity of the ternary component structure to understand its thermal property. Then, we find two different camouflage mechanisms (thermal magnifier and external cloak) with some certain requirements of the ternary component structure. Concretely speaking, the thermal magnifier can disguise a small object into a big one, and the external cloak can hide a component outside the cloak. The mechanisms proposed in this work are completely different from the transformation scheme[1–6] and bilayer scheme.[7–9]

II. THEORY

We explore the thermal properties of a ternary component structure by calculating its effective thermal conductivity. First, we consider a two-dimensional ternary component structure embedded in a matrix [see Fig. 1(a)]. The core and two shells have the radius r_1, r_2, and r_3 with the thermal conductivities κ_1, κ_2, and κ_3, respectively. The thermal conductivity of the matrix is κ_4. In this model, the core and two shells are anisotropic. κ_1, κ_2, and κ_3 are tensors in cylindrical coordinates (r, θ), and κ_4 is a scalar.

The effective thermal conductivity of the core and the first shell is[23,24]

$$\kappa_{12} = c_2 \kappa_{rr2} \frac{c_1 \kappa_{rr1} + c_2 \kappa_{rr2} + (c_1 \kappa_{rr1} - c_2 \kappa_{rr2}) p_1^{c_2}}{c_1 \kappa_{rr1} + c_2 \kappa_{rr2} - (c_1 \kappa_{rr1} - c_2 \kappa_{rr2}) p_1^{c_2}} \quad (1)$$
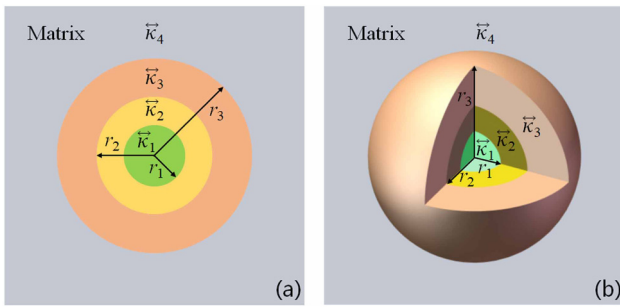
FIG. 1. Schematic diagram of a (a) two-dimensional and (b) three-dimensional ternary component structure.

and that of the ternary component structure can be calculated by the iteration method,

$$\kappa_{123} = c_3 \kappa_{rr3} \frac{\kappa_{12} + c_3 \kappa_{rr3} + (\kappa_{12} - c_3 \kappa_{rr3}) p_2^{c_3}}{\kappa_{12} + c_3 \kappa_{rr3} - (\kappa_{12} - c_3 \kappa_{rr3}) p_2^{c_3}}, \quad (2)$$

where $\boldsymbol{\kappa}_i = \mathrm{diag}(\kappa_{rri}, \kappa_{\theta\theta i})$, $p_i = (r_i/r_{i+1})^2$, and $c_i = \sqrt{\kappa_{\theta\theta i}/\kappa_{rri}}$.

Especially, when Eq. (2) satisfies the following two relations,

$$c_2 \kappa_{rr2} + c_3 \kappa_{rr3} = 0, \quad (3)$$

$$p_1^{c_2} - p_2^{c_3} = 0, \quad (4)$$

it can be reduced as

$$\kappa_{123} = c_1 \kappa_{rr1}. \quad (5)$$

Equations (3)–(5) can be reduced to the isotropic condition with $c_1 = c_2 = c_3 = 1$,

$$\kappa_{rr2} + \kappa_{rr3} = 0, \quad (6)$$

$$p_1 - p_2 = 0, \quad (7)$$

$$\kappa_{123} = \kappa_{rr1}. \quad (8)$$

Secondly, we explore the three-dimensional ternary component structure [see Fig. 1(b)]. The effective thermal conductivity of the core and the first shell is[23,24]

$$\kappa_{12} = \kappa_{rr2} \frac{u_{21}(u_{11}\kappa_{rr1} - u_{22}\kappa_{rr2}) - u_{22}(u_{11}\kappa_{rr1} - u_{21}\kappa_{rr2}) p_1^{(u_{21}-u_{22})/3}}{(u_{11}\kappa_{rr1} - u_{22}\kappa_{rr2}) - (u_{11}\kappa_{rr1} - u_{21}\kappa_{rr2}) p_1^{(u_{21}-u_{22})/3}} \quad (9)$$

and that of the ternary component structure can be calculated by the iteration method,

$$\kappa_{123} = \kappa_{rr3} \frac{u_{31}(\kappa_{12} - u_{32}\kappa_{rr3}) - u_{32}(\kappa_{12} - u_{31}\kappa_{rr3}) p_2^{(u_{31}-u_{32})/3}}{(\kappa_{12} - u_{32}\kappa_{rr3}) - (\kappa_{12} - u_{31}\kappa_{rr3}) p_2^{(u_{31}-u_{32})/3}}, \quad (10)$$

where $\boldsymbol{\kappa}_i = \mathrm{diag}(\kappa_{rri}, \kappa_{\theta\theta i}, \kappa_{\varphi\varphi i})$ with $\kappa_{\theta\theta i} = \kappa_{\varphi\varphi i}$ for simplicity, $p_i = (r_i/r_{i+1})^3$, and $u_{i1,2} = \left(-1 \pm \sqrt{1 + 8\kappa_{\theta\theta i}/\kappa_{rri}}\right)/2$.

Especially, when Eq. (10) satisfies the following two relations,

$$u_{21}\kappa_{rr2} - u_{32}\kappa_{rr3} = 0, \quad (11)$$

$$p_2^{(u_{31}-u_{32})/3}(u_{31} - u_{32}) \left[(\kappa_{rr1}u_{11}u_{21} - \kappa_{rr2}u_{21}u_{22}) + \frac{p_1^{(u_{21}-u_{22})/3}}{2}(\kappa_{rr1}u_{11} - \kappa_{rr2}u_{21}) \right]$$
$$+ p_1^{(u_{21}-u_{22})/3}(u_{21} - u_{22}) \left[(\kappa_{rr1}u_{11}u_{32} - \kappa_{rr2}u_{21}u_{31}) + \frac{p_2^{(u_{31}-u_{32})/3}}{2}(\kappa_{rr1}u_{11} - \kappa_{rr2}u_{21}) \right] = 0, \quad (12)$$

it can be reduced as

$$\kappa_{123} = \kappa_{rr1}u_{11}. \quad (13)$$

Equations (11)–(13) can be reduced to the isotropic condition with $u_{11} = u_{21} = u_{31} = 1$,

$$\kappa_{rr2} + 2\kappa_{rr3} = 0, \quad (14)$$

$$p_2 \left[(\kappa_{rr1} + 2\kappa_{rr2}) + \frac{p_1}{2}(\kappa_{rr1} - \kappa_{rr2}) \right]$$
$$+ p_1 \left[(-2\kappa_{rr1} - \kappa_{rr2}) + \frac{p_2}{2}(\kappa_{rr1} - \kappa_{rr2}) \right] = 0, \quad (15)$$

$$\kappa_{123} = \kappa_{rr1}. \quad (16)$$

Equations (3)–(5) and (11)–(13) are the key results obtained in this work.

III. TWO APPLICATIONS OF THE TERNARY COMPONENT STRUCTURE

A. Thermal magnifier: Disguising a small object into a big one

The object size can be reflected by its distinct external temperature distribution. When a small anisotropic object is put into a matrix [see Fig. 2(a)], the temperature distribution is present in Fig. 2(d). Then, we wrap it up with an anisotropic shell, and a ternary component structure is completed (with the matrix inside the dashed circle) [see Fig. 2(b)]. When the
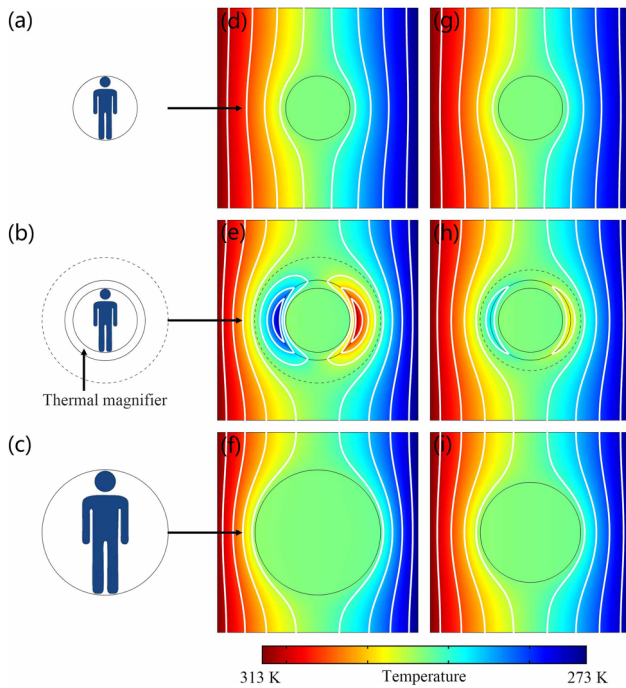
FIG. 2. Two-dimensional (a)–(c) schematic diagram, (d)–(f) anisotropic condition [Eqs. (3) and (4)], and (g)–(i) isotropic condition [Eqs. (6) and (7)] of thermal magnifier. Dashed circles in (b), (e), and (h) are plotted for comparison with (c), (f), and (i), respectively. (a)–(c) figuratively demonstrate that a small object (a) can be disguised into a large one (c) by a thin external shell (b) without changing the original thermal conductivity. Concrete parameters: (d)–(i) the size of simulation box is 16×16 cm, with background thermal conductivity $\kappa_4 = 1 \, \text{W m}^{-1} \text{K}^{-1}$. (d) A core with $r_1 = 2.56$ cm and $\kappa_1 = \text{diag}(\mathbf{25}, \mathbf{100}) \, \text{W m}^{-1} \text{K}^{-1}$. (e) The core is wrapped up with a shell with $r_2 = 3.2$ cm and $\kappa_2 = \text{diag}(-0.5, \, -2) \, \text{W m}^{-1} \text{K}^{-1}$. (f) A comparative core with $r_3 = 4$ cm and thermal conductivity with $\kappa_3 = \text{diag}(25, 100) \, \text{W m}^{-1} \text{K}^{-1}$. (g) A core with $r_1 = 2.56$ cm, and $\kappa_1 = 50 \, \text{W m}^{-1} \text{K}^{-1}$. (h) The core is wrapped up with a shell with $r_2 = 3.2$ cm and $\kappa_2 = -1 \, \text{W m}^{-1} \text{K}^{-1}$. (i) A comparative core with $r_3 = 5$ cm, and thermal conductivity with $\kappa_3 = 50 \, \text{W m}^{-1} \text{K}^{-1}$. White lines represent isotherms.

ternary component structure satisfies the requirement of Eqs. (3) and (4), it possesses the same external temperature distribution [Fig. 2(e)] with a big anisotropic object [Fig. 2(f)]. Therefore, we disguise a small object into a big one.

The above discussions are for anisotropic conditions. When the material we use is isotropic, the problem can be reduced. The results are similar to those of anisotropic conditions [see Figs. 2(g)–2(i)]. To be mentioned, the object sizes in Figs. 2(f) and 2(i) are different, which means that anisotropy can manipulate how big the small object is disguised. Such a scheme has potential applications in infrared misleading, such as camouflaging the object sizes.

Three-dimensional schemes are also explored in Fig. 3. Anisotropic results and isotropic results are, respectively, shown in Figs. 3(a)–3(c) and 3(d)–3(f). The same temperature distribution between Figs. 3(b) and 3(c) [or 3(e) and 3(f)]

validates the proposed scheme, which indicates that a small object is disguised into a big one in three dimensions.

B. External cloak: Hiding a component outside the cloak

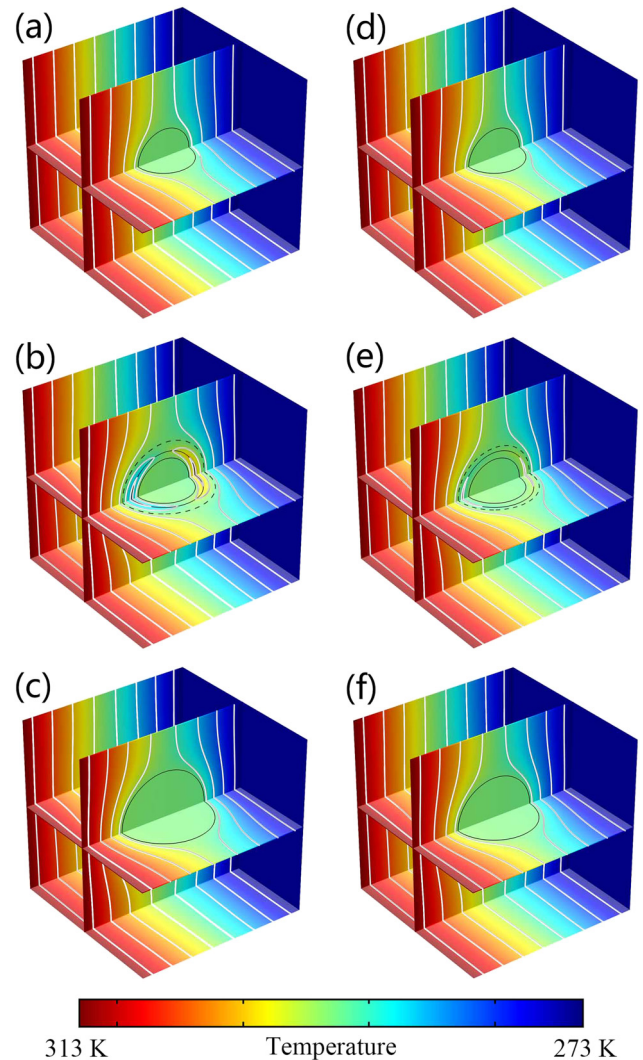The thermal conductivity of a component can be reflected by its distinct external temperature distribution.

FIG. 3. Three-dimensional (a)–(c) anisotropic condition [Eqs. (11) and (12)] and (d)–(f) isotropic condition [Eqs. (14) and (15)] of thermal magnifier. Concrete parameters: (a)–(f) the size of simulation box is $16 \times 16 \times 16$ cm, with background thermal conductivity $\kappa_4 = 1 \, \text{W m}^{-1} \text{K}^{-1}$. (a) A core with $r_1 = 2.56$ cm and $\kappa_1 = \text{diag}(25, 75, 75) \, \text{W m}^{-1} \text{K}^{-1}$. (b) The core is wrapped up with a shell with $r_2 = 3.2$ cm and $\kappa_2 = \text{diag}(-0.5, \, -1.5, \, -1.5) \, \text{W m}^{-1} \text{K}^{-1}$. (c) A comparative core with $r_3 = 3.62$ cm, and thermal conductivity with $\kappa_3 = \text{diag}(25, 75, 75) \, \text{W m}^{-1} \text{K}^{-1}$. (d) A core with $r_1 = 2.56$ cm and $\kappa_1 = 50 \, \text{W m}^{-1} \text{K}^{-1}$. (e) The core is wrapped up with a shell with $r_2 = 3.2$ cm and $\kappa_2 = -2 \, \text{W m}^{-1} \text{K}^{-1}$. (f) A comparative core with $r_3 = 4.15$ cm, and the thermal conductivity with $\kappa_3 = 50 \, \text{W m}^{-1} \text{K}^{-1}$.

When an anisotropic component is put into a matrix [see Fig. 4(a)], it will present the temperature distribution in Fig. 4(d). Then, we embed an anisotropic core into the component, and a ternary component structure is completed [see Fig. 4(b)]. When the ternary component structure satisfies the requirement of Eqs. (3) and (4), it possesses the same external temperature distribution [Fig. 4(e)] with the "Null" object [Fig. 4(f)]. In other words, the component is hidden outside the cloak. "Null" is similar to the thermal transparency in Ref. 12, but we realize the phenomenon with different mechanism, say, ternary component structure.

When we simplify the anisotropic problem to the isotropic one, there is no change of the results. To be mentioned, the sizes of the embedded cores in Figs. 4(e) and 4(h) are different, which means that anisotropy can manipulate the size of the external cloak. Such a scheme has potential

applications in protecting objects from being detected by infrared camera.

We also explore the three-dimensional schemes (see Fig. 5). Anisotropic results and isotropic results are, respectively, shown in Figs. 5(a)–5(c) and 5(d)–5(f). The same uniform
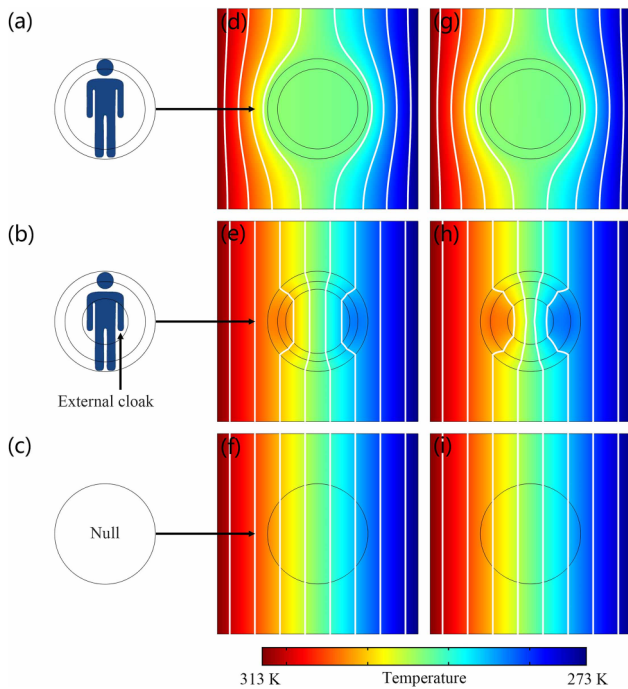

FIG. 4. Two-dimensional (a)–(c) schematic diagram, (d)–(f) anisotropic condition [Eqs. (3) and (4)], and (g)–(i) isotropic condition [Eqs. (6) and (7)] of external cloak. (a)–(c) figuratively demonstrate that a composite (a) can be camouflaged into "Null" (c) by an internal core (b) with the same thermal conductivity of background. Concrete parameters: (d)–(i) the size of simulation box is 16×16 cm, with background thermal conductivity $\kappa_4 = 1$ W m^{-1} K^{-1}. (d) A core with $r_2 = 3.2$ cm and $\kappa_2 = \mathrm{diag}(62.5, 40)$ W m^{-1} K^{-1}, and a shell with $r_3 = 4$ cm and $\kappa_3 = \mathrm{diag}(-25, -100)$ W m^{-1} K^{-1}. (e) The core-shell is filled with an internal core with $r_1 = 2.56$ cm and $\kappa_1 = \mathrm{diag}(1.25, 0.8)$ W m^{-1} K^{-1}. (f) A comparative core with radius 4 cm and thermal conductivity 1 W m^{-1} K^{-1}. (g) A core with $r_2 = 3.2$ cm and $\kappa_2 = 50$ W m^{-1} K^{-1}, and a shell with $r_3 = 4$ cm and $\kappa_3 = -50$ W m^{-1} K^{-1}. (h) The core-shell is filled with an internal core with $r_1 = 1.83$ cm and $\kappa_1 = 1$ W m^{-1} K^{-1}. (i) A comparative core with radius 4 cm and thermal conductivity 1 W m^{-1} K^{-1}.
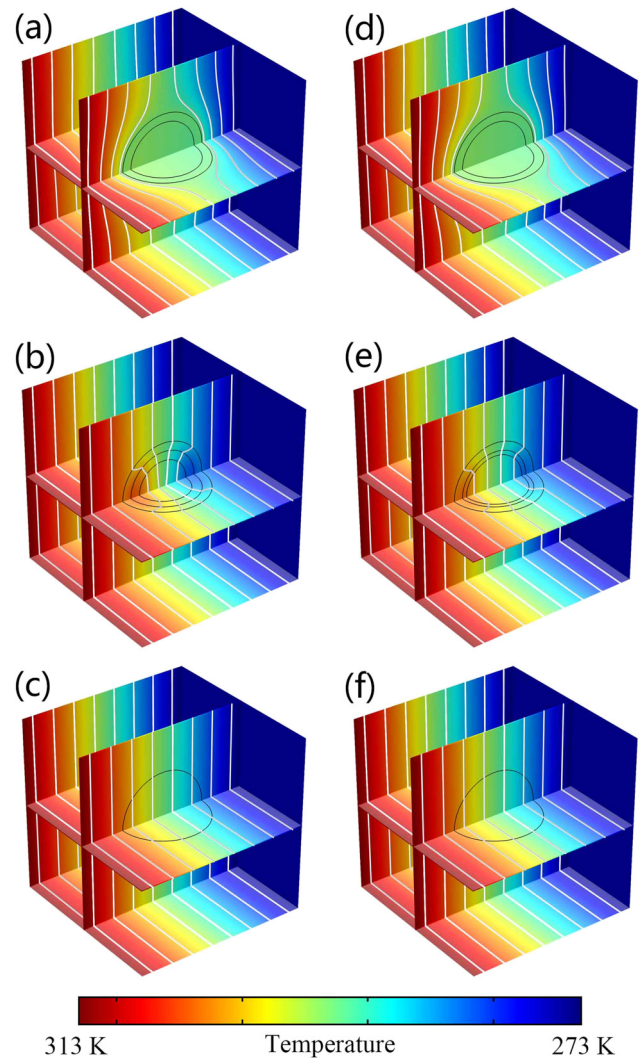
FIG. 5. Three-dimensional (a)–(c) anisotropic condition [Eqs. (11) and (12)] and (d)–(f) isotropic condition [Eqs. (14) and (15)] of external cloak. Concrete parameters: (a)–(f) the size of simulation box is $16 \times 16 \times 16$ cm, with background thermal conductivity $\kappa_4 = 1$ W m^{-1} K^{-1}. (a) A core with $r_2 = 3.2$ cm and $\kappa_2 = \mathrm{diag}(62.5, 45, 45)$ W m^{-1} K^{-1}, and a shell with $r_3 = 4$ cm and $\kappa_3 = \mathrm{diag}(-50/3, -50, -50)$ W m^{-1} K^{-1}. (b) The core-shell is filled with an internal core with $r_1 = 2.8$ cm and $\kappa_1 = \mathrm{diag}(1.25, 0.9, 0.9)$ W m^{-1} K^{-1}. (c) A comparative core with radius 4 cm and thermal conductivity 1 W m^{-1} K^{-1}. (d) A core with $r_2 = 3.2$ cm and $\kappa_2 = 50$ W m^{-1} K^{-1}, and a shell with $r_3 = 4$ cm and $\kappa_3 = -25$ W m^{-1} K^{-1}. (e) The core-shell is filled with an internal core with $r_1 = 2.36$ cm and $\kappa_1 = 1$ W m^{-1} K^{-1}. (f) A comparative core with radius 4 cm and thermal conductivity 1 W m^{-1} K^{-1}.

temperature gradient between Figs. 5(b) and 5(c) [or 5(e) and 5(f)] indicates that a component outside the cloak can be hidden in three dimensions.

IV. DISCUSSION AND CONCLUSION

Despite the novel phenomena, the two proposed functions require apparent negative thermal conductivity, including controlled external energy.[25–27] Apparent negative thermal conductivity means that the direction of heat flux is from low temperature to high temperature, which violates the second law of thermodynamics. To solve this problem, adding external energy is a good method. In this way, the direction of heat flux can be from low temperature to high temperature without violating the second law of thermodynamics and hence apparent negative thermal conductivity is realized. For experimental realization, the point heat sources can be achieved by following the experimental setup adopted in Fig. 1, Ref. 28. To validate the feasibility, we take the thermal magnifier shown in Fig. 2(h) as an example. We set the thermal conductivity of the shell to be positive, and then add line heat sources [Fig. 6(a)] and point heat sources [Fig. 6(b)], respectively. The same temperature distributions with Fig. 2(h) show that the active materials do work.

Nevertheless, the proposed thermal magnifier and external cloak are well-behaved in steady states because we do not consider the role of densities and heat capacities. Certainly, such a thermal magnifier and external cloak in transient states are promising as well, and good results can be expected due to the pioneering works on transient states.[4,13,29]

In summary, we have designed a ternary component structure and calculated its effective thermal conductivity.

By deriving the specific relations for the ternary component structure, we proposed two distinct camouflage phenomena, i.e., thermal magnifier and external cloak. Such schemes have potential applications in misleading the infrared detection, such as size camouflage and invisibility. The corresponding mechanisms can be directly extended to other diffusive fields,[30–32] such as electrostatic, magnetostatic, and particle diffusive fields.
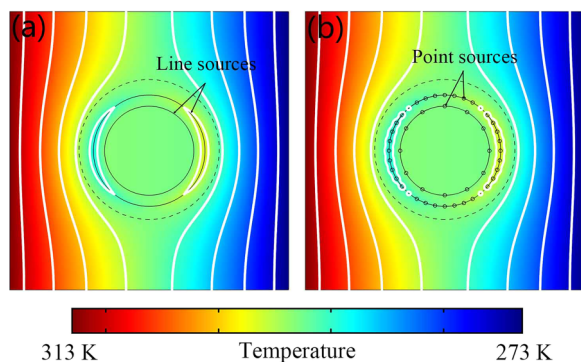
FIG. 6. Realization of apparent negative thermal conductivity by adding (a) line sources and (b) point sources. The parameter settings are the same as those in Fig. 2(h) except for the shell. The thermal conductivity of the shell is set to be positive $1 \, W \, m^{-1} \, K^{-1}$. (a) Line sources are applied which obey the temperature distribution $T = 3.75x - 25.6x/r_{1,2}^2 + 293$, where r_1 (r_2) is applied for the inner (outer) boundary of the shell. x represents the abscissa whose origin is located in the middle of the simulation box. (b) Twelve discontinuous sources (with radius 0.1 cm) and 36 discontinuous sources (with radius 0.1 cm) are, respectively, applied on the inner and outer boundaries of the shell. The point temperatures are calculated from the temperature distribution in (a) according to the source positions.

REFERENCES

[1]C. Z. Fan, Y. Gao, and J. P. Huang, "Shaped graded materials with an apparent negative thermal conductivity," Appl. Phys. Lett. **92**, 251907 (2008).

[2]T. Y. Chen, C. N. Weng, and J. S. Chen, "Cloak for curvilinearly anisotropic media in conduction," Appl. Phys. Lett. **93**, 114103 (2008).

[3]J. Y. Li, Y. Gao, and J. P. Huang, "A bifunctional cloak using transformation media," J. Appl. Phys. **108**, 074504 (2010).

[4]S. Guenneau, C. Amra, and D. Veynante, "Transformation thermodynamics: Cloaking and concentrating heat flux," Opt. Express **20**, 8207 (2012).

[5]S. Narayana and Y. Sato, "Heat flux manipulation with engineered thermal materials," Phys. Rev. Lett. **108**, 214303 (2012).

[6]R. Schittny, M. Kadic, S. Guenneau, and M. Wegener, "Experiments on transformation thermodynamics: Molding the flow of heat," Phys. Rev. Lett. **110**, 195901 (2013).

[7]H. Y. Xu, X. H. Shi, F. Gao, H. D. Sun, and B. L. Zhang, "Ultrathin three-dimensional thermal cloak," Phys. Rev. Lett. **112**, 054301 (2014).

[8]T. C. Han, X. Bai, D. L. Gao, J. T. L. Thong, B. W. Li, and C. W. Qiu, "Experimental demonstration of a bilayer thermal cloak," Phys. Rev. Lett. **112**, 054302 (2014).

[9]Y. G. Ma, Y. C. Liu, M. Raza, Y. D. Wang, and S. L. He, "Experimental demonstration of a multiphysics cloak: Manipulating heat flux and electric current simultaneously," Phys. Rev. Lett. **113**, 205501 (2014).

[10]S. Guenneau and C. Amra, "Anisotropic conductivity rotates heat fluxes in transient regimes," Opt. Express **21**, 6578 (2013).

[11]T. C. Han, X. Bai, J. T. L. Thong, B. W. Li, and C. W. Qiu, "Full control and manipulation of heat signatures: Cloaking, camouflage and thermal metamaterials," Adv. Mater. **26**, 1731 (2014).

[12]T. Z. Yang, X. Bai, D. L. Gao, L. Z. Wu, B. W. Li, J. T. L. Thong, and C. W. Qiu, "Invisible sensors: Simultaneous sensing and camouflaging in multiphysical fields," Adv. Mater. **27**, 7752 (2015).

[13]T. Z. Yang, Y. Su, W. Xu, and X. D. Yang, "Transient thermal camouflage and heat signature control," Appl. Phys. Lett. **109**, 121905 (2016).

[14]Y. Li, X. Bai, T. Z. Yang, H. Luo, and C. W. Qiu, "Structured thermal surface for radiative camouflage," Nat. Commun. **9**, 273 (2018).

[15]R. Hu, S. L. Zhou, Y. Li, D. Y. Lei, X. B. Luo, and C. W. Qiu, "Illusion thermotics," Adv. Mater. **30**, 1707237 (2018).

[16]S. L. Zhou, R. Hu, and X. B. Luo, "Thermal illusion with twinborn-like heat signatures," Int. J. Heat Mass Transfer **127**, 607 (2018).

[17]L. J. Xu, R. Z. Wang, and J. P. Huang, "Camouflage thermotics: A cavity without disturbing heat signatures outside," J. Appl. Phys. **123**, 245111 (2018).

[18]L. J. Xu and J. P. Huang, "A transformation theory for camouflaging arbitrary heat sources," Phys. Lett. A **382**, 3313 (2018).

[19]K. P. Vemuri and P. R. Bandaru, "Anomalous refraction of heat flux in thermal metamaterials," Appl. Phys. Lett. **104**, 083901 (2014).

[20]T. Z. Yang, K. P. Vemuri, and P. R. Bandaru, "Experimental evidence for the bending of heat flux in a thermal metamaterial," Appl. Phys. Lett. **105**, 083908 (2014).

[21]K. P. Vemuri, F. M. Canbazoglu, and P. R. Bandaru, "Guiding conductive heat flux through thermal metamaterials," Appl. Phys. Lett. **105**, 193904 (2014).

[22]R. S. Kapadia and P. R. Bandaru, "Heat flux concentration through polymeric thermal lenses," Appl. Phys. Lett. **105**, 233903 (2014).

[23]S. Yang, L. J. Xu, R. Z. Wang, and J. P. Huang, "Full control of heat transfer in single-particle structural materials," Appl. Phys. Lett. **111**, 121908 (2017).

[24]R. Z. Wang, L. J. Xu, Q. Ji, and J. P. Huang, "A thermal theory for unifying and designing transparency, concentrating and cloaking," J. Appl. Phys. **123**, 115117 (2018).

[25]M. Wegener, "Metamaterials beyond optics," Science **342**, 939 (2013).

[26]Y. Gao and J. P. Huang, "Unconventional thermal cloak hiding an object outside the cloak," Eur. Phys. Lett. **104**, 44001 (2013).

[27]X. Y. Shen and J. P. Huang, "Thermally hiding an object inside a cloak with feeling," Int. J. Heat Mass Transfer **78**, 1 (2014).

[28]D. M. Nguyen, H. Y. Xu, Y. M. Zhang, and B. L. Zhang, "Active thermal cloak," Appl. Phys. Lett. **107**, 121901 (2015).

[29]S. R. Sklan, X. Bai, B. W. Li, and X. Zhang, "Detecting thermal cloaks via transient effects," Sci. Rep. **6**, 32915 (2016).

[30]F. Gomory, M. Solovyov, J. Souc, C. Navau, J. P. Camps, and A. Sanchez, "Experimental realization of a magnetic cloak," Science **335**, 1466 (2012).

[31]R. M. Batlle, A. Parra, S. Laut, N. D. Valle, C. Navau, and A. Sanchez, "Magnetic illusion: Transforming a magnetic object into another object by negative permeability," Phys. Rev. Appl. **9**, 034007 (2018).

[32]W. Jiang, Y. G. Ma, and S. L. He, "Static magnetic cloak without a superconductor," Phys. Rev. Appl. **9**, 054041 (2018).